

EUROPEAN ORGANIZATION FOR NUCLEAR RESEARCH

Proposal to the ISOLDE and Neutron Time-of-Flight Committee

Beta-delayed neutron emission of ^{134}In and search for $i_{13/2}$ single particle neutron state in ^{133}Sn

13/05/2020

R. Grzywacz^{1,2}, M. Madurga¹, M. Karny³, A. Algora⁴, J.M. Allmond², D. Bardayan⁵, J. Benito⁶, N. Brewer², A. Fijałkowska³, L.P. Gaffney⁷, J. Heideman¹, S. Neupane¹, T. King¹, N. Kitamura¹, L. M. Fraile⁶, M. J. Garcia Borge⁸, A. Illana^{9,10}, Z. Janas³, K.L. Jones¹, T. Kawano¹¹, K. Kolos¹², A. Korgul³, R. Lică¹³, C. Mazzocchi³, K. Miernik³, J.R. Murias⁶, R.D. Page⁷, M. Piersa³, B.C. Rasco², M.M. Rajabali¹⁴, K. Rykaczewski², K. Siegl¹, M. Singh¹, C. Sotty⁸, O. Tengblad⁸, N. Warr¹⁵, H. DeWitte¹⁶, R. Yokoyama¹, Z. Xu¹

¹Dept. of Physics and Astronomy, University of Tennessee, Knoxville, Tennessee 37996, USA.

² Physics Division, Oak Ridge National Laboratory, Oak Ridge, Tennessee 37830, USA.

³ Faculty of Physics, University of Warsaw, PL 00-681 Warsaw, Poland.

⁴ Instituto de Física Corpuscular, Edificio de Institutos de Paterna, E-46071 Valencia, Spain.

⁵ Institute for Structure and Nuclear Astrophysics, Department of Physics, Notre Dame, Indiana 46556, USA.

⁶ Grupo de Física Nuclear & IPARCOS, Universidad Complutense de Madrid, E-28040, Spain.

⁷ The University of Liverpool, Liverpool L69 7ZE, United Kingdom.

⁸ Instituto de Estructura de la Materia, E-28006 Madrid, Spain.

⁹ University of Jyväskylä, Department of Physics, Jyväskylä, Finland

¹⁰ Helsinki Institute of Physics, Helsinki, Finland

¹¹ Theoretical Division, Los Alamos National Laboratory, Los Alamos, NM 87545, USA

¹² Lawrence Livermore National Laboratory, Livermore, California 94550, USA.

¹³ National Institute of Physics and Nuclear Engineering, RO-077125 Bucharest, Romania

¹⁴ Tennessee Technological University, Cookeville, Tennessee, USA

¹⁵ Institut für Kernphysik, Universität zu Köln, Germany.

¹⁶ KU Leuven, Instituut voor Kern-en Stralingsfysica, 3001 Leuven, Belgium.

Spokesperson(s): Robert Grzywacz (University of Tennessee, ORNL), rgrzywac@utk.edu,
Miguel Madurga (University of Tennessee), Miguel.madurga@gmail.com
Marek Karny (University of Warsaw), Marek.Karny@fuw.edu.pl
Local contact: Razvan Lică (razvan.lica@cern.ch)

Abstract

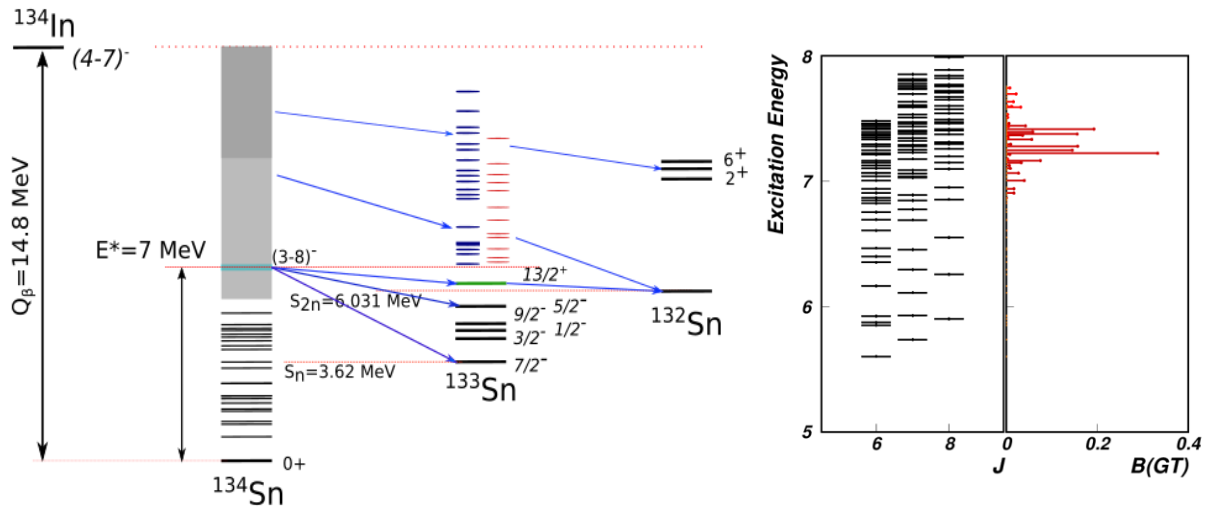
We propose to study beta-delayed neutron emission from ^{134}In using Isolde Decay Station neutron and gamma detectors and new high-resolution neutron detector NEXT. The experiment aims to perform high-statistics and high-resolution spectroscopy of neutrons, which are emitted from excited states in ^{134}Sn and ^{133}Sn . The experiment addresses multiple goals relevant to nuclear structure and astrophysics. It will provide data which will constrain the models of beta decays and statistical particle emission near ^{132}Sn . The focus of this experiment will be to study two-neutron emission from excited states in ^{134}Sn . The relatively large probability of this process



will enable the identification of the neutron single-particle $i_{13/2}$ state in ^{133}Sn , which will be populated in the neutron emission from ^{134}Sn ; it is predicted to be neutron unbound.

Requested shifts: 18 shifts

Introduction: The decays of nuclei near doubly-magic ^{132}Sn are essential to understand the fundamentals of the beta-delayed neutron emission process due to the relative simplicity of the underlying nuclear structure. This enables a credible comparison of the nuclear model predictions and experimental data. The critical problem in modeling beta-decay using modern configuration-interaction theory is the very extensive valence space needed due to the large proton-neutron asymmetry, which is computationally challenging. This is the case for the majority of the very neutron-rich nuclei of interest, for example, those on the r-process nucleosynthesis path. A consequence of the large decay energies of the parent and small neutron separation in the daughter is that beta-delayed neutron emission is the dominant decay channel for most of the very neutron-rich nuclei. This two-step process requires the knowledge of the beta-decay feeding pattern in the first stage, and neutron and gamma emission mechanism in the second stage [Kaw08, Mum16]. The probability distribution of both processes is determined by the underlying nuclear structure of involved nuclei. Beta decays of such few, and unique nuclei such as $^{79,80}\text{Co} \rightarrow ^{79,80}\text{Ni}$ or $^{133,134}\text{In} \rightarrow ^{133,134}\text{Sn}$ are critical to benchmark nuclear models far from stability. Presently experiments with indium isotopes are feasible [Hof96,Dil-2,Pie20], while the cobalt decay



studies did not reach beyond $N=50$ [Xu14] due to small production cross-section.

Figure 1. Beta decay of ^{134}In . The excited neutron unbound states in ^{134}Sn will decay via neutron emission to neutron bound and unbound states in ^{133}In . The hypothetical $13/2^+$ state in ^{133}Sn is marked green. Its excitation energy is expected to be below 3 MeV, which will enable its population in the decay of neutron unbound states with energies above 6.6 MeV in ^{134}Sn . (Right) Shell-model predictions for the negative excited states in ^{134}Sn and Gamow-Teller strength distribution using modified interactions [Yua16] with added orbitals outside $N=82$ neutron shell gap. The calculations were done for the $J=7^-$ spin and parity of the ^{134}In ground state

The continuous development of improved laser ionization schemes at ISOLDE [Han00,Dil02] enables the production of these isotopes with high rates, enabling spectroscopic studies of even very small decay branches. Recently we studied the beta-delayed neutron emission from the ^{133}In precursor [Mad17,Xu20]. The unique use of RILIS

allowed for selectively ionize the $9/2^+$ ground state and $1/2^-$ isomer. The results from our recent experiment on beta delayed neutron emission from ^{133}In and $^{133\text{m}}\text{In}$ decays provided a very complete data set [Xu20]. This is a very typical r-process beta-delayed neutron precursor: the decays of $N>82$ and $Z=49$ indiums have very large Q_β values and their beta decay populates tin isotopes with small neutron separation energy. We were able to observe and quantify the dominant Gamow-Teller transformation of the neutron $g_{7/2}$ into a $g_{9/2}$ proton, the primary goal of that experiment. The experiment observed intense first forbidden (FF) transitions connecting various single-particle levels in this very proton-neutron asymmetric nucleus. Due to the paucity of bound excited states in ^{133}Sn we observed multiple strong individual transitions to neutron unbound states in ^{133}Sn . The observed transition probabilities were consistent with the shell-model predictions [Yos18] using a large valence space in protons and neutrons. Additionally, we observed direct neutron emission from known gamma decaying states [Pie19,Vaq17]. This demonstrates that the neutron or gamma-ray emission occurs from very narrow states with sub-keV widths even at very high excitation energies where neutron emission widths are naively expected to be large.

The data analysis of this experiment is completed and the first publication is in preparation [Xu20]. The natural next step of this investigation, neutron and gamma-ray spectroscopy of ^{134}In decay is proposed here. Identical nuclear structure effects will determine the general decay properties of ^{134}In . However, the details of the decay of ^{134}In are different than those in the decay of ^{133}In . Main difference comes from the small two-neutron separation energy of ^{134}Sn . It opens up of populating neutron-unbound states in ^{133}Sn with very different spin and parities of those in the beta-decay of ^{133}In , under the compound nucleus assumption [Kaw08]. ^{134}In is an odd-odd nucleus, with a high-spin ground state most likely $J^\pi=(4^- - 7^-)$ from the coupling of the three valence neutrons outside $N=82$ closed shell. They are most likely in the $f_{7/2}$ neutron orbital coupled to the $g_{9/2}$ proton hole in $Z=50$. The beta-decay ground state energy is high, about $Q_\beta=14.7$ MeV, and the decay daughter ^{134}Sn has low one- and two-neutron separation energies $S_n=3.6$ MeV and $S_{2n}=6.03$ MeV respectively. The expected Gamow-Teller decay will be of the same nature as in ^{133}In ($vg_{7/2} \rightarrow \pi g_{9/2}$ $E^* \sim 6$ MeV). Due to the odd-even effect the GT resonance is predicted to be at 7 MeV energy in ^{134}In , similar to the ^{132}In decay. This excited state is therefore predicted to be above the two-neutron separation energy, which opens up exciting possibilities for investigating states in ^{133}Sn . Besides, the presence of two valence neutrons outside the $N=82$ closed shell, leads to a much higher density of excited states in ^{134}Sn , which may be reflected in the observed beta-decay properties. In addition, neutrons will be emitted to bound excited states in ^{133}Sn [Hof96], with relatively well-established spin assignments [Jon12] which can be used to aid in spin assignment of intermediate in states in ^{134}In . In ^{133}In decay neutrons emitted from excited states in ^{133}Sn proceed almost entirely to the ground state of ^{132}Sn due to the high-energy of the first excited state.

The experiment will attempt a detailed study of neutron and gamma-ray spectroscopy using IDS neutron time-of-flight array and IDS clover detectors required for proper reconstruction of the level scheme. In addition, we will complement this system with NEXT neutron array [Hei19], which will provide the capability for much-improved resolution of neutron energy measurement in addition to neutron-gamma discrimination capability. This is achieved by adding neutron interaction localization capability achieved via segmentation of the array.

Goals of experiments: The decay of βn precursor ^{134}In will address multiple goals, which all can be achieved in a single measurement with the IDS experimental setup.

The first goal will be a measurement of the main Gamow-Teller decay channel $\nu g_{7/2} \rightarrow \pi g_{9/2}$, via its neutron emission. Our recent shell-model calculation predicts that this transformation will populate a group of states at about 7 MeV, which are one and two-neutron unbound, see Figure 1. The decay of this group of resonances can be complicated. In the case of single neutron emission, the excited single-particle states in ^{133}Sn will be populated. This will lead to fragmentation of the neutron spectrum and will require neutron-gamma coincidence measurement. Figure 2 summarizes the predictions from the Los Alamos Hauser Feshbach(HF) CoH3 code [Kaw16, Kaw19] of the relative intensities of neutron and gamma rays in the decay of a single 7 MeV state in ^{134}Sn for different spins assuming compound nucleus [Kaw08]. Neutron emission probabilities are only determined by the optical model parameters and not details of the structure (wave functions) of the nuclear states. This measurement is essential to establish systematics of the GT quenching near

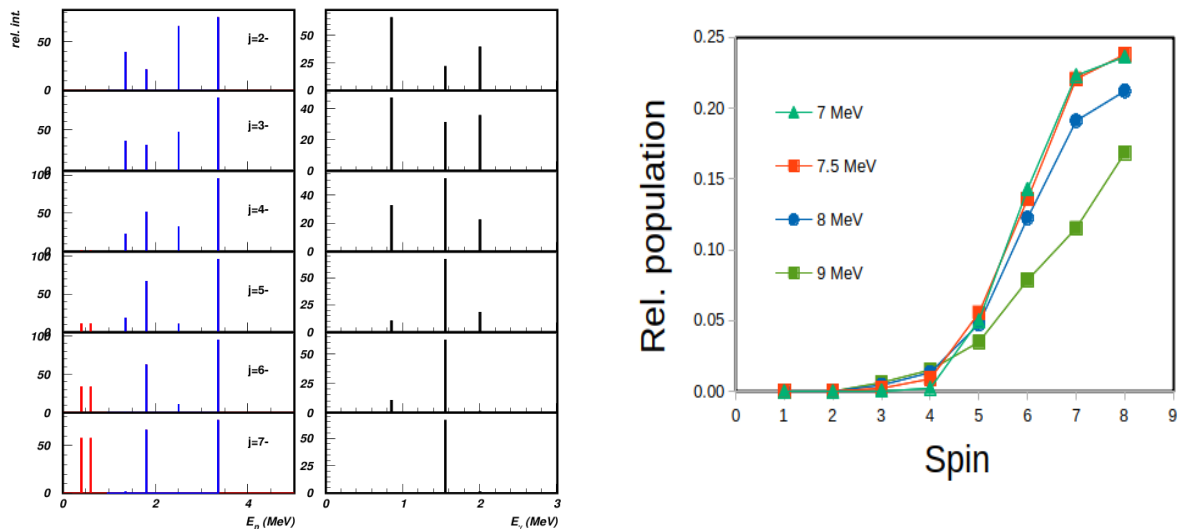


Figure 2. Neutron (red and blue) and gamma-ray (black) spectra simulated using the CoH3 Hauser-Feshbach code [Kaw16] from the single excited state at $E^*=7$ MeV in ^{134}In , with Koning-Delaroche optical model parameters. The neutron energies marked in red are from two-neutron emission populating a hypothetical $i_{13/2}$ state at $E=2791$ keV in the left panels. (Right) Relative population of the $13/2^+$ state as a function of spin and E^* of the neutron emitting state in ^{134}Sn .

doubly magic nuclei. It is required to benchmark recently developed nuclear theories [Gys19] and compare them to e.g. future the charge-exchange experiments when they become feasible beyond ^{132}Sn [Yas18]. The understanding of the relative importance of GT and forbidden transitions in the neutron-rich nuclei is needed to make credible global predictions for the r-process nuclei [Mol03].

The second goal of this experiment is the measurement of two-neutron emission probabilities from the excited states in ^{134}Sn . The ^{134}Sn has low two-neutron separation energy and offers a unique opportunity to study this process, such as energy correlations between neutrons. This has never been done in a heavy nucleus and is an excellent test of the parameterization of optical models of neutron emission within the HF formalism. We will use the information from our previous experiment to perform neutron-neutron coincidence measurement and thus identify two-neutron emitting excited states in ^{134}Sn populated in the ^{134}In beta decay. This will enable a more complete determination of the beta-decay strength distribution. In addition to two-neutron emission, two-neutron unbound states are known to decay via emission of a single neutron [Yok19, Mol19]. This is correctly predicted by CoH3 statistical model, see Figure 2. For most of them we were able to make a tentative spin

assignments based on their population intensity in the decay of ^{133}In ground state ($J=9/2^+$) and isomer ($J=1/2^-$) [Xu20] and this will enable a very detailed comparison with the statistical model predictions. The use of NEXT detector is essential, thanks to its high-resolution energy measurement capability. NEXT will focus on isolating known transition from ^{133}In decay, while the IDS Neutron DETector (INDiE) will provide high-efficiency to detect neutron emitting states in ^{134}Sn precursor.

The third goal of this experiment is the identification of the $i_{13/2}$ single-particle neutron state in ^{133}Sn . The $13/2^+$ neutron single-particle state in ^{133}Sn is predicted to be neutron-unbound and is expected below 3 MeV excitation energy [Urb99,Lei14]. It was sought for in a direct reaction experiment [All14]. A possible candidate was found at 2791 keV via observation of a single gamma-ray in a neutron transfer experiment [All14], but this assignment was deemed inconclusive by the authors. This was due to the expected dominant neutron decay channel from this state, which would overwhelm the E3 gamma-decay channel. The relative population of the $i_{13/2}$ state in the neutron transfer reaction would have been unexpectedly large for the observation of 2791 keV line. In the proposed experiment, we will search for the $i_{13/2}$ state, which is very likely to be populated in the neutron emission from ^{134}Sn excited states. The expected high-spin ground-state of ^{134}In is a key factor in achieving this goal, see Figure 2. The excited states populated in ^{134}Sn via GT or FF transition will be predominantly high-spin. Neutron emission from ^{134}Sn unbound states will also preferentially populate high-spin states in ^{133}Sn due to the smaller centrifugal barrier in the emission of a neutron with low orbital angular momentum. This decay scenario was modeled using the HF CoH3 code [Kaw16]. In these calculations we have tentatively placed the $13/2^+$ excited state in ^{133}Sn at $E^*=2791$ keV and calculated neutron spectra for various excitation energies of the excited states in ^{134}Sn . In this scenario, a neutron line at $E^*-S_n=392$ keV will be observed for the emission from ^{133}Sn , the other neutron, emitted from excited states in ^{134}Sn , will carry the energy which will depend on the energy of excited state in ^{134}Sn . The signature of the $i_{13/2}$ state will be (here) a neutron line at about 400 keV in coincidence with higher energy neutrons from excited states in ^{134}Sn , which are feeding this state.

The fourth goal of this proposal will be direct identification of the proton-core breaking transitions, which will populate states at about 10 MeV excitation energy. The previous measurement by the Warsaw University group showed that excited states, including the 6^+ isomer, in ^{132}Sn are populated [Pie20]. In order to explain this observation a population of states in ^{134}Sn , which are at least about 10 MeV in excitation energy, is required. We plan also to devote a short measurement with ^{132}In ($J^\pi=7^-$, $Q_\beta=14.14$ MeV, $P_{\text{ln}}=6.3\%$). The GT transition is populating neutron bound state at $E^*=7.2$ MeV ($S_n=7.353$ MeV) and proton-core excitations will be decaying via single neutron emission.

Experimental setup: The experiment will be instrumented at the ISOLDE Decay Station using its standard set of 4 clover detectors, $\sim 4\%$ efficiency at 1 MeV, the IDS in-vacuum beta detector, 90% electron detection efficiency, and the newly commissioned IDS Neutron DETector (INDiE) using VANDLE array detector design and electronics [Pau14,Pet16]. The angular acceptance for 26 bars at 100 cm is $\Omega=11\%$ of 4π , and using 90% beta efficiency, the total efficiency of the array is between 3-5%, see Figure 3. The performance of this system was demonstrated during the ^{133}In decay experiment. The neutron detection will be enhanced by 15 NEXT neutron detector modules, which will have much higher neutron energy resolution due to their segmentation and provide additional 3% neutron detection efficiency. These detectors are capable for neutron-gamma discrimination above

400 keV neutron energy, which is an added benefit for this measurement. These detectors will be operated at 50 cm TOF and will be placed on both sides of INDiE. Both detectors have a neutron detection threshold of about 100 keV. During the ^{133}In experiment (IS630), we performed a short production test of ^{134}In which resulted in a preliminary neutron spectrum demonstrating the feasibility of the proposed measurement.

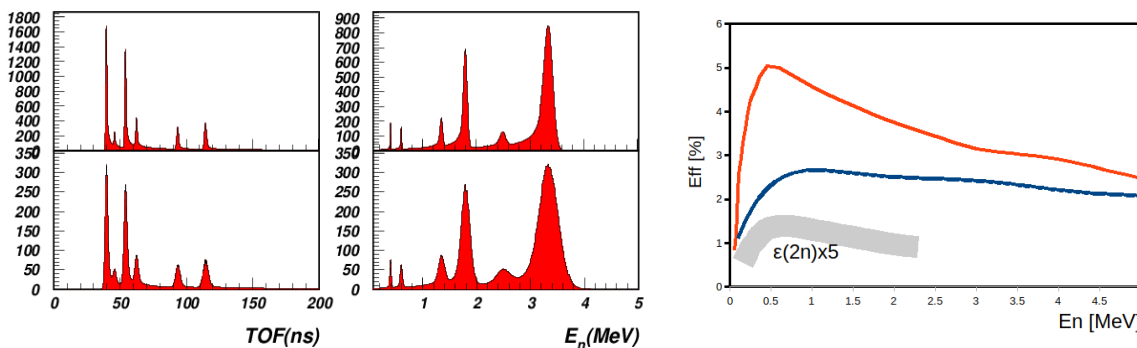


Figure 3. (left) Simulated neutron spectra for NEXT (top) and INDiE (bottom) detectors for the excitation of the 7 MeV with e.g. $J=5^-$ (see Figure 2). Two low energy peaks are from the 2n decay proceeding via the hypothetical $13/2^+$ state in ^{133}Sn . (Right) The neutron detection efficiencies: (red) INDiE consisting of 26 modules at 100 cm. (blue) NEXT for 16 modules at 50 cm TOF. (grey) Estimated two-neutron detection efficiency (multiplied by 5) for $E_{1n}=E_{2n}$ situation. The NEXT detector covers approximately half of the solid angle compared to that of INDiE.

Summary of requested shifts:

Table 1: Expected neutron rates. These calculations are done for 2 uC PS Booster beam and 50% transmission efficiency to IDS (*n.c.* = neutron converter)

| | P_{1n} (%) | Yield (ion/ μC) | IDSND Eff | Neutrons (1/h) | Shifts | Target | Source |
|-------------------|-----------------|--------------------------------|--------------|-------------------|--------|---------------------------|--------------------------------|
| ^{132}In | 6.3% | 8000 | 0.04 | $4.0 \cdot 10^4$ | 2 | $\text{UC}_X+\text{n.c.}$ | Hot Ta line and cavity + RILIS |
| ^{134}In | 80% | 100 | 0.04 | $8.1 \cdot 10^3$ | 15 | $\text{UC}_X+\text{n.c.}$ | Hot Ta line and cavity + RILIS |
| ^{17}N | 95.1% | 100 | 0.04 | $1.0 \cdot 10^5$ | 1 | CaO | Hot Ta line and cavity |

Table 1 summarizes the requested beam time. Due to the lack of beta-decaying isomers in even In isotopes, we request the hot Ta ion source along with the RILIS ion source in broadband mode. Enhancement of In release using RILIS has been observed in several experiments at ISOLDE [Dil02,Fra16], with yields of 8000 and 95 ions/uC for ^{132}In and ^{134}In respectively. The main isobaric components, and therefore contamination, in masses 132 and 134 are the relatively long-lived isotopes of iodine and cesium. However, these are not neutron emitters; therefore they will not contribute to the background in INDiE. In the case of ^{134}In , the daughter ^{134}Sn has a neutron branching ratio of 17%. Recent experiments at IDS [Fra16,Mad17] showed an effectively complete suppression of Sn components using a combination of electromagnetic separation and RILIS. We request 15 shifts to collect at least 1×10^6 neutrons from the decay of ^{134}In and two shifts to collect about 0.5×10^6 neutrons from ^{132}In . The calculations were made using the measured spectrum of ^{134}In convoluted with known neutron detection efficiency. The more recent preliminary estimates from BRIKEN data of $P_{1n}=0.8$ and $P_{2n}=0.1$ were used [Est17]. During the 20 shifts we expect to collect about 15×10^3 of two-neutron events. This number carries about 50% uncertainty due

to unknown spectrum of the neutrons observed in this process. Beam time breaks down in 2 shifts for ^{132}In , 15 shifts for ^{134}In and 1 shift for ^{17}N calibration. Measured spectra of ^{133}In and ^{134}In will be provided to INTC.

References:

- [All0] J. Allmond et al. Phys. Rev. Lett. 112, 172701 (2014).
- [Dil02] I. Dillmann, et al., Eur. Phys. J. A **13** (2002) 281.
- [Est17] A. Estrade et al. BRIKEN collaboration, RIBF proposal, private communication.
- [Fra16] L.M. Fraile, ISOLDE HRS eLogBook, June 9th (2016).
- [Gys19] A.R. Gysbers et al. Nature Physics volume 15, 425–426(2019).
- [Han00] M. Hannawald et al. Phys.Rev. **C62**, 054301 (2000).
- [Hei19] J. Heideman, Nuclear Instruments and Methods A, 946 (2019) 162528.
- [Hof96] P. Hoff et al., Phys. Rev. Lett. **77**, 1020 (1996).
- [Jon10] K.L. Jones et al., Nature **465**, 454 (2010).
- [Kaw08] T. Kawano, P. Moller, and W. B. Wilson, Phys. Rev. C **78**, 054601 (2008).
- [Kaw19] T. Kawano, <https://arxiv.org/abs/1901.05641>.
- [Kaw16] T. Kawano, R. Capote, S. Hilaire, and P. Chau Huu-Tai, Phys. Rev. C **94**, 014612 ((2016).
- [Lei14] Y. Lei and H. Jiang, Phys. Rev. C **90**, 047305 (2014).
- [Mad17] M. Madurga, ISOLDE GPS eLogBook, April 29th (2017).
- [Mad16] M. Madurga et al., Phys. Rev. Lett. **117**, 092502 (2016).
- [Mol03] P. Möller, B. Pfeiffer and K. L. Kratz. Phys. Rev. C **67**, 055802, (2003).
- [Mol19] Möller et al., Atomic Data and Nuclear Data Tables **125**, 1-192 (2019).
- [Mum16] M. R. Mumpower, T. Kawano, and P. Möller Phys. Rev. C **94**, 064317 (2016).
- [Pau14] S. Paulauskas et al., Nuclear Instruments and Methods A **737**, 22 (2014).
- [Pet16] W. Peters et al. Nuclear Instruments and Methods A **836**, 122 (2016).
- [Pie18] M. Piersa et al. Phys. Rev. C **99**, 024304 (2019).
- [Pie20] M. Piersa et al. to be submitted (2020).
- [Urb99] W. Urban, et al., Eur. Phys. J. A **5**, 239 (1999).
- [Vaq17] V. Vaquero, et al., Phys. Rev. Lett. **118**, 202502 (2017).
- [Yok19] R. Yokoyama et al., Phys. Rev C **100**(3), 031302(R) (2019).
- [Yos18] S. Yoshida et al. Phys. Rev. C **97**, 054321 (2018).
- [Yas18] J. Yasuda et al. Phys. Rev. Lett., **121**, 132501 (2018).
- [Yua16] C. Yuan et al. Physics Letters B **762**, 237 (2016).
- [Xu20] Z.Y. Xu et al. to be submitted (2020).
- [Xu14] Z.Y. Xu et al. Phys. Rev. Lett. **113**, 032505(2014).

Appendix

DESCRIPTION OF THE PROPOSED EXPERIMENT

The experimental setup comprises: *(name the fixed-ISOLDE installations, as well as flexible elements of the experiment)*

| Part of the Choose an item. | Availability | Design and manufacturing |
|--|--|---|
| [if relevant, name fixed ISOLDE installation: COLLAPS, CRIS, ISOLTRAP, MINIBALL + only CD, MINIBALL + T-REX, NICOLE, SSP-GLM chamber, SSP-GHM chamber, or WITCH] | <input checked="" type="checkbox"/> Existing | <input checked="" type="checkbox"/> To be used without any modification |
| | IDS | To be used as currently existing |
| [Part 1 of experiment/ equipment] | <input type="checkbox"/> Existing | <input type="checkbox"/> To be used without any modification <input type="checkbox"/> To be modified |
| | <input type="checkbox"/> New | <input type="checkbox"/> Standard equipment supplied by a manufacturer <input type="checkbox"/> CERN/collaboration responsible for the design and/or manufacturing |
| [Part 2 experiment/ equipment] | <input type="checkbox"/> Existing | <input type="checkbox"/> To be used without any modification <input type="checkbox"/> To be modified |
| | <input type="checkbox"/> New | <input type="checkbox"/> Standard equipment supplied by a manufacturer <input type="checkbox"/> CERN/collaboration responsible for the design and/or manufacturing |
| [insert lines if needed] | | |

HAZARDS GENERATED BY THE EXPERIMENT

(if using fixed installation) Hazards named in the document relevant for the fixed [COLLAPS, CRIS, ISOLTRAP, MINIBALL + only CD, MINIBALL + T-REX, NICOLE, SSP-GLM chamber, SSP-GHM chamber, or WITCH] installation.

Additional hazards:

| Hazards | | | |
|---------------------------------------|---------------------------------------|--------------------------------------|--------------------------------------|
| | [Part 1 of the experiment/equipment] | [Part 2 of the experiment/equipment] | [Part 3 of the experiment/equipment] |
| Thermodynamic and fluidic | | | |
| Pressure | [pressure][Bar], [volume][l] | | |
| Vacuum | | | |
| Temperature | [temperature] [K] | | |
| Heat transfer | | | |
| Thermal properties of materials | | | |
| Cryogenic fluid | [fluid], [pressure][Bar], [volume][l] | | |
| Electrical and electromagnetic | | | |
| Electricity | [voltage] [V], [current][A] | | |
| Static electricity | | | |
| Magnetic field | [magnetic field] [T] | | |
| Batteries | <input type="checkbox"/> | | |
| Capacitors | <input type="checkbox"/> | | |
| Ionizing radiation | | | |

| | | | |
|--|---|--|--|
| Target material | [material] | | |
| Beam particle type (e, p, ions, etc) | | | |
| Beam intensity | | | |
| Beam energy | | | |
| Cooling liquids | [liquid] | | |
| Gases | [gas] | | |
| Calibration sources: | <input type="checkbox"/> | | |
| • Open source | <input type="checkbox"/> | | |
| • Sealed source | <input type="checkbox"/> [ISO standard] | | |
| • Isotope | | | |
| • Activity | | | |
| Use of activated material: | | | |
| • Description | <input type="checkbox"/> | | |
| • Dose rate on contact and in 10 cm distance | [dose][mSV] | | |
| • Isotope | | | |
| • Activity | | | |
| Non-ionizing radiation | | | |
| Laser | | | |
| UV light | | | |
| Microwaves (300MHz-30 GHz) | | | |
| Radiofrequency (1-300MHz) | | | |
| Chemical | | | |
| Toxic | [chemical agent], [quantity] | | |
| Harmful | [chemical agent], [quantity] | | |
| CMR (carcinogens, mutagens and substances toxic to reproduction) | [chemical agent], [quantity] | | |
| Corrosive | [chemical agent], [quantity] | | |
| Irritant | [chemical agent], [quantity] | | |
| Flammable | [chemical agent], [quantity] | | |
| Oxidizing | [chemical agent], [quantity] | | |
| Explosiveness | [chemical agent], [quantity] | | |
| Asphyxiant | [chemical agent], [quantity] | | |
| Dangerous for the environment | [chemical agent], [quantity] | | |
| Mechanical | | | |
| Physical impact or mechanical energy (moving parts) | [location] | | |
| Mechanical properties (Sharp, rough, slippery) | [location] | | |
| Vibration | [location] | | |
| Vehicles and Means of Transport | [location] | | |
| Noise | | | |
| Frequency | [frequency],[Hz] | | |
| Intensity | | | |
| Physical | | | |
| Confined spaces | [location] | | |
| High workplaces | [location] | | |
| Access to high workplaces | [location] | | |
| Obstructions in passageways | [location] | | |
| Manual handling | [location] | | |
| Poor ergonomics | [location] | | |

0.1 Hazard identification

3.2 Average electrical power requirements (excluding fixed ISOLDE-installation mentioned above):
(make a rough estimate of the total power consumption of the additional equipment used in the experiment)

The INDiE detectors run at 1000 V and use 1 mA current on average, drawing 1 W each. The next detector have exactly the same power requirements. We will run 40 detectors, requiring 40 W.